Structural Engineering and Mechanics, *Vol. 55, No. 4 (2015) 801-813*
DOI: http://dx.doi.org/10.12989/sem.2015.55.4.801

Equivalent moment of inertia of a truss bridge with steel-concrete composite deck

Wojciech Siekierski*

Institute of Civil Engineering, Poznań University of Technology, ul. Piotrowo 5, 61-138 Poznań, Poland

(Received April 23, 2015, Revised July 16, 2015, Accepted July 25, 2015)

Abstract. Flexural stiffness of bridge spans has become even more important parameter since Eurocode 1 introduced for railway bridges the serviceability limit state of resonance. For simply supported bridge spans it relies, in general, on accurate assessment of span moment of inertia that governs span flexural stiffness. The paper presents three methods of estimation of the equivalent moment of inertia for such spans: experimental, analytical and numerical. Test loading of the twin truss bridge spans and test results are presented. Recorded displacements and the method of least squares are used to find an "experimental" moment of inertia. Then it is computed according to the analytical method that accounts for joint action of truss girders and composite deck as well as limited span shear stiffness provided by diagonal bracing. Finally a 3D model of finite element method is created to assess the moment of inertia. Discussion of results is given. The comparative analysis proves efficiency of the analytical method.

Keywords: moment of inertia; truss bridge; steel-concrete composite deck; joint action; shear stiffness

1. Introduction

Flexural stiffness is one of crucial parameters of a bridge span. For a long time it has governed the serviceability limit state of deflection of a bridge superstructure. European standard of bridge design introduced another limit state that depends on the parameter. It is the serviceability limit state for railway bridge spans concerning hazard of resonance induced by crossing trains.

Estimation of bridge span flexural stiffness is relatively easy for plate-girder and box-girder bridges. Their cross-section is coherent-all components are tied together continually along span length. It is so particularly for modern bridges which exhibit joint action of main girders and a deck. Arch, cable-stayed and suspension bridges have complex cross-sections. In all these cases components that influence span flexural stiffness are connected at some points along the span by members that are "weak" along the span (hangers). Moreover, for suspension bridges and cable-stayed bridges, construction of pylons influences span flexural stiffness. Truss-girder bridge spans differ from the two groups. Their components are separated in cross-section but connected with a bracing system that is relatively rigid along span length. The differences are shown in Fig. 1.

The paper compares estimations of moment of inertia for a truss bridge span based on testing, finite element method and analytical method. The latter one takes into account joint action of the

*Corresponding author, Ph.D., E-mail: wojciech.siekierski@put.poznan.pl

http://www.techno-press.org/?journal=sem&subpage=8 ISSN: 1225-4568 (Print), 1598-6217 (Online)

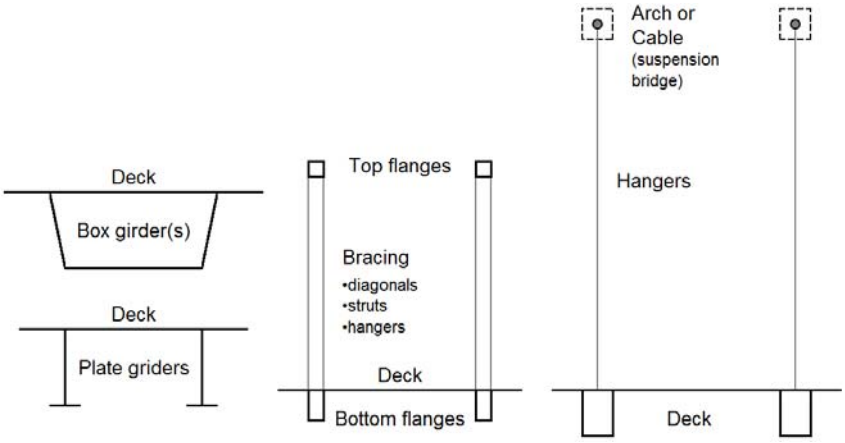

Fig. 1 Cross-sections of bridge spans

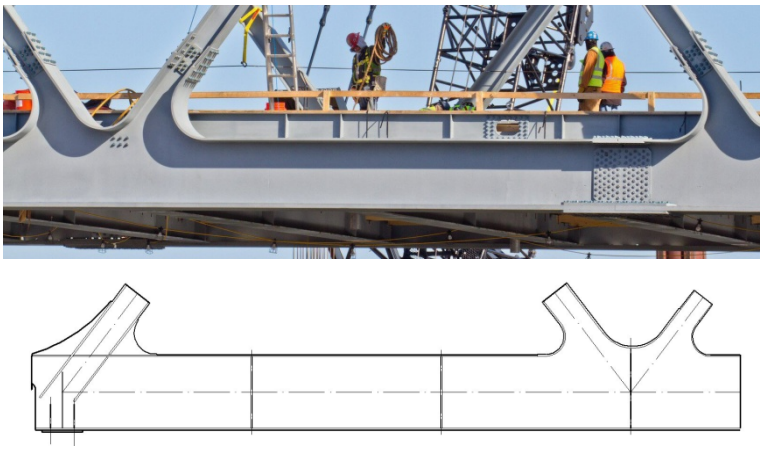

Fig. 2 Bottom flange of a gussetless bridge truss girder (top) and an example of assembly part (bottom)

bridge deck and girders as well as limited shear stiffness provided by diagonal bracing. It is applicable to preliminary design of trussed structures and rapid assessment of flexural stiffness of existing truss bridge spans.

2. Trussed structures in bridge building

Bridge building still applies trussed structures to carry loads. The most popular are truss girders characterized recently by Chen *et al*. (2013), Unsworth (2010). Modern bridge truss girders are usually gussetless-gusset plates are incorporated into member vertical walls (Fig. 2). Thus nodes are truly rigid. In terms of static behaviour the girders act as frames and as such they are analysed.

Besides having rigid nodes the bridge trussed structures more and more often carry loads applied at nodes and between them (Fig. 3). Such truss bridge spans are described for instance by Reintjes (2009) as well as Xia and Zhong (2011).

Trussed systems are widely used also as main members of decks of arched and cable-stayed

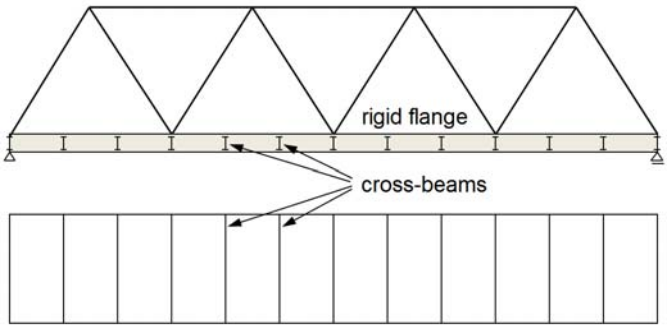

Fig. 3 The idea of modern truss bridge span

Fig. 4 Examples of contemporary bridge decks: steel-concrete composite (left) and orthotropic (right); both shown for I and box cross-sections of the flange of trussed structure

bridges. Such structures are reported by Xia and Zhong (2011), Zhang and Zhang (2011), Zheng and Dai (2013) as well as Nan *et al*. (2014). They are also applied as stiffening members of decks of suspension bridges as described by Li *et al*. (2007).

Due to cross-beam arrangement shown in Fig. 3 the flanges of trussed structures carry significant bending moments. So the flanges usually have cross-section of significant height to get an appropriate moment of inertia. I-sections and box-sections are used. To reduce dimensions of joints the flange members are usually situated eccentrically in reference to their theoretical flange axes.

The decks of simply supported or suspended to arches or pylons trussed structures are similar The idea is shown in Fig. 4- concrete slabs and steel orthotropic decks are used. The joint action of the decks and main girders is usually expected. In railway bridges the decks carry regular railway tracks (rails, slippers, gravel).

3. Tested bridge spans and test loading results

Twin bridge spans, shown in Fig. 5, were tested. Geometrical data of the spans:
- theoretical span length: 51.0 m,
- truss girder spacing: 5.30 m,
- truss girder theoretical height: 8.00 m,
- distance between centres of gravity of top and bottom flanges: 8.85 m,
- bottom flange node spacing: 12.75 m,
- cross-beam spacing: 3.19 m,
- RC slab thickness – variable – 0.25÷0.33 m

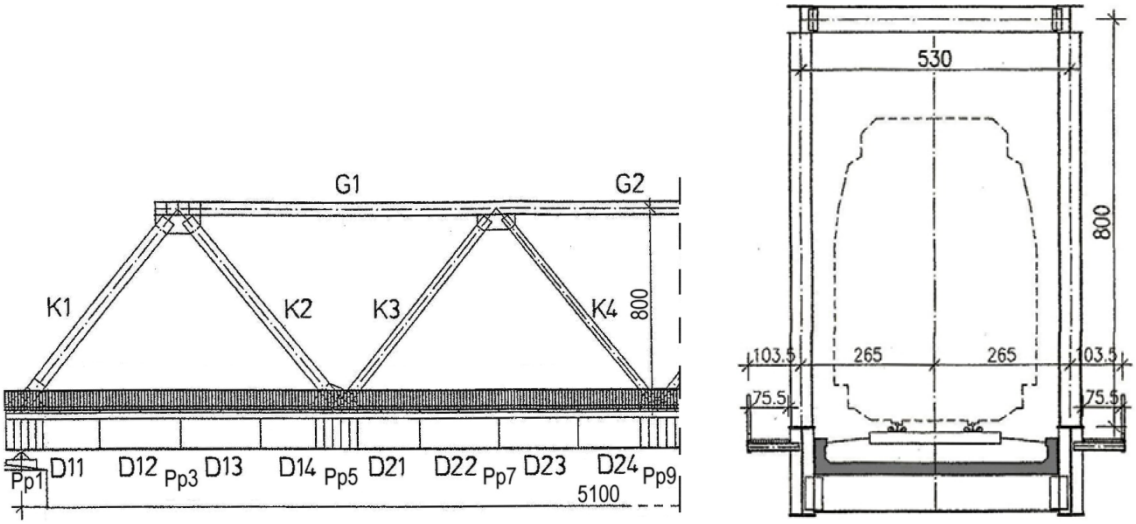

Fig. 5 Analyzed bridge span: general view (left) and cross-section (right)

Table 1 Cross-section characteristics of main structural elements

Model element (for symbols see Fig. 5)	A_X (cm^2)	I_X (cm^4)	I_Y (cm^4)	I_Z (cm^4)
D11, D12 (half of length near D11)	364	231	1669197	33358
D12 (half of length near D13), D13, D14 (half of length near D13),	394	337	1878496	39608
D14 (half of length near D21), D21 (half of length near D14)	474	794	2466298	56274
D21 (half of length near D22), D22÷D24	310	432	158183	41711
G1	405	958	221373	58398
G2	244	243	87208	37514
K1	184	110	25014	59471
K2	134	58	12803	40572
K3	98	32	4503	27393
K4	170	150	5439	15719
Transverse beam – composite beam	599	57000	614000	810000
Transverse beam – steel beam	364	231	1669197	33358
Concrete slab	8 shell elements across and 32 shell elements along the deck slab, 28 cm thick			

- slab longitudinal reinforcement: top and bottom layers of 32 ϕ25 steel bars.

Cross-sectional characteristics, according to the design documentation, are given in Table 1.

For the testing of both spans the same set of three coupled locomotives was used-Fig. 6. In the case of both spans, railway track is located symmetrically between truss girders (Fig. 5).

Vertical displacements of bottom flange nodes 1, 2 and 3 (Fig. 6) were recorded during testing. The land survey method used for measuring provided accuracy of 0.01 mm. The recorded displacements are put together in Table 2. Positive sign marks direction downwards.

Because of the similarity of loading conditions for the four girders (I-A, I-B, II-A and II-B)

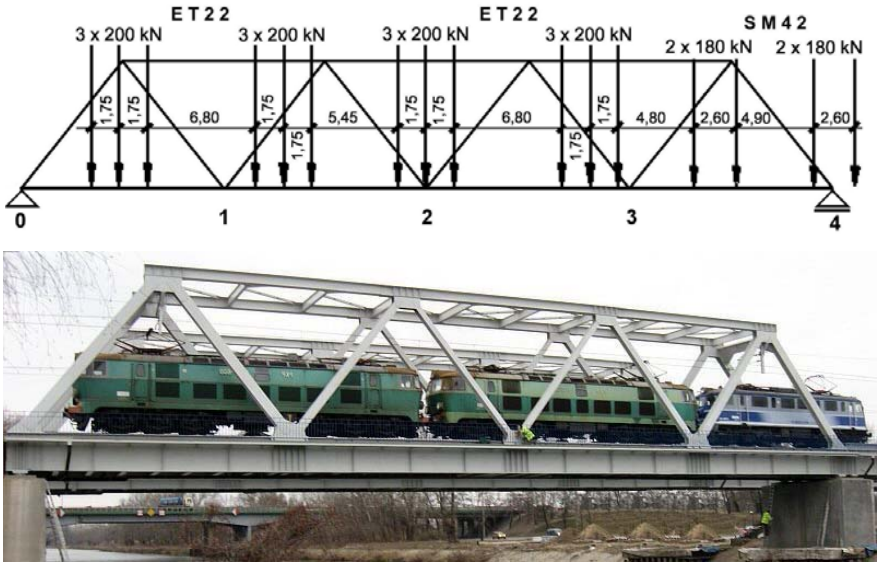

Fig. 6 Test loading: scheme (top) and general view (bottom)

Table 2 Elastic displacements of truss bottom flange nodes

Flange node (i)	Location	Elastic displacement (mm)			
		Span I		Span II	
		girder I-A (k=1)	girder I-B (k=2)	girder II-A (k=3)	girder II-B (k=4)
1	¼·L_t	8.05	8.25	8.15	8.20
2	½·L_t	11.35	12.10	11.85	11.80
3	¾·L_t	7.65	8.25	8.30	8.20

their node displacement recordings, given in Table 2, were assumed to be statistic samples (four samples per flange node). Mean values of displacements at flange nodes are computed according to the equation

$$u_{i\,ave} = \frac{\sum_{k=1}^{n} u_{ik}}{n} \tag{1}$$

where: $u_{i\,ave}$-mean value of the displacement of node i, i=1, 2, 3, u_{ik}-the k-th sample of recorded displacements at the node i, k=1, 2, 3, 4, n-number of samples, n=4.

Standard deviation for the mean values of displacements, given in Table 3, is computed according to the equation

$$s_i = \sqrt{\frac{\sum_{k=1}^{n}\left(u_{ik} - u_{i\,ave}\right)^2}{n-1}} \quad . \tag{2}$$

The computed mean displacements and standard deviations computed for population of four samples are put together in Table 3. It can be seen from Table 3 that the scatter of recorded

Table 3 Mean displacements and standard deviations

Flange node (i)	Location	Mean elastic displacement $u_{i\,ave}$ (mm)	Standard deviation s_i (mm)	s_i / $u_{i\,ave}$
1	¼·L_t	8.16	0.09	1%
2	½·L_t	11.78	0.34	3%
3	¾·L_t	8.10	0.33	4%

displacements for each node is small-standard deviation up to 4% of the respective mean value. It supports the preliminary assumptions that the four truss girders are treated as four statistic samples.

4. Experimental estimation of span moment of inertia

The estimation is based on recorded node displacements. The method of least squares is chosen to find an equivalent moment of inertia of truss bridge spans. It is the most popular statistical method being applied in practice. Its implementation in a spreadsheet is fairly easy. For direct measurements with average Gauss error equal to zero (as land survey repeatable measurements) the criterion of least squares method is equivalent to the criterion of the highest credibility method.

The equivalent moment of inertia of the tested truss bridge spans is defined as the one that provides the following

$$\sum_{i=1}^{3}\left(u_{i\,rec}-u_{i\,est}\right)^2=\min \tag{3}$$

where: $u_{i\,rec}$-recorded displacement of nodes of truss bottom flange (Table 3), $u_{i\,est}$-displacement of the respective three points located on a simply supported beam of equivalent moment of inertia and of the bridge span length.

Displacements $u_{i\,est}$ of a simply supported beam of equivalent moment of inertia are computed as superposition of displacement of respective point "i" caused by the nodal forces P_j-resultants of division of forces shown in Fig. 6 into bottom flange nodes (0, 1, 2, 3, 4). The method of computing node displacements is shown in Fig. 7.

Vertical displacement u_{ij} of flange node "i" caused by the nodal force P_j equals (Fig. 7)

$$\begin{aligned}
&\text{if } x_i \le x_j: \quad u_{ij\,est}=\frac{P_j\cdot\left(L_t-x_j\right)\cdot x_i\cdot\left[L_t^{\,2}-\left(L_t-x_j\right)^2-x_i^{\,2}\right]}{6\cdot E\cdot J_{TR}\cdot L_t}\\
&\text{if } x_i > x_j: \quad u_{ij\,est}=\frac{P_j\cdot x_j\cdot\left(L_t-x_i\right)\cdot\left[L_t^{\,2}-x_j^{\,2}-\left(L_t-x_i\right)^2\right]}{6\cdot E\cdot J_{TR}\cdot L_t}
\end{aligned} \tag{4}$$

where: x_i and x_j are ordinates of node "i" and concentrated load P_j along rigid flange, respectively (Fig. 7), L_t-theoretical span length, i.e., distance between axes of supports (m), E-elastic modulus of steel (kPa), J_{TR}-moment of inertia of equivalent simply supported beam representing a bridge span (m^4).

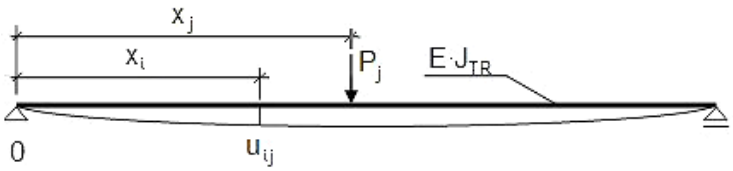

Fig. 7 Method of computing displacement of an equivalent beam

Table 4 Computed displacements for the equivalent moment of inertia I_{exp}

Nodal forces P_j (kN)	Displacements $u_{ij\ est}$ (mm) at the respective points on the equivalent beam		
	1 (¼·L_t)	2 (½·L_t)	3 (¾·L_t)
P_0=305.4	0.00	0.00	0.00
P_1=742.8	2.62	3.20	2.03
P_2=839.6	3.61	5.26	3.61
P_3=736.4	2.02	3.17	2.59
P_4=315.8	0.00	0.00	0.00
Total ($u_{i\ est}$)	8.24	11.62	8.24

Total displacement of flange node "*i*" is

$$u_{i\ est} = \sum_{j=1}^{3} u_{ij\ est} \tag{5}$$

Nodal forces P_j were computed. Then the equivalent moment of inertia I_{exp} for the experimental results ($u_{i\ rec}$) was computed with an aid of a result search analysis available in a spreadsheet, under the condition given in Eq. (3). During the process estimated displacements were computed as in Eq. (4). The nodal forces P_j and displacements of respective points (1, 2, 3) of an equivalent simply supported beam They are put together in Table 4.

The obtained equivalent moment of inertia for bridge span equals I_{exp}=2,154 m^4.

5. Analytical method of estimation of span moment of inertia

5.1 Simplified technique

Simple technique of estimation of moment of inertia in bending for through truss bridge span is computing it as total moment of inertia of two truss girders

$$I_{a.s} = 2 \cdot \left(I_t + A_t \cdot z_t^{\ 2} + I_b + A_b \cdot z_b^{\ 2} \right) \tag{6}$$

where: $I_{a.s}$-moment of inertia in bending for a truss bridge span (m^4), I_t, I_b-average moments of inertia of top and bottom flange of a truss girder, respectively (m^4), A_t, A_b-average cross-sectional area of top and bottom flange of a truss girder, respectively (m^2), z_t, z_b-distance from the truss centre of gravity to the centre of gravity of top and bottom flange of a truss girder, respectively (m).

Location of the truss centre of gravity is computed as follows

Table 5 The computation results of the simple analytical method

Parameter	Units	Value
A_b	m^2	0.0423
I_b	m^4	0.0210
A_t	m^2	0.0342
I_t	m^4	0.0018
z_b	m	3.95
z_t	m	4.90
$I_{a.s}$	m^4	3.007

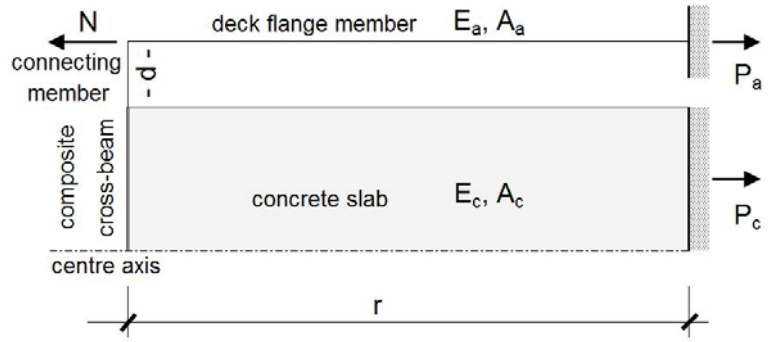

Fig. 8 Structural system for setting equivalent cross-sectional area of flange member adjacent to deck

$$z_b = \frac{A_t \cdot h_t}{A_t + A_b}$$
$$z_t = h_t - z_b \tag{7}$$

where: h_t-distance between top and bottom flange centre of gravity.

The computation results of the simple analytical method, applied to the truss bridge span described in the Chapter 3, are put together in Table 5.

5.2 Refined technique

The technique accounts for influence of bridge deck and limited shear stiffness provided by diagonal bracing. Accounting for influence of steel-concrete composite deck on flexural stiffness of through truss bridge span is described by Siekierski (2014). It is based on the idea of an equivalent cross-sectional area of members of truss flange adjacent to the composite deck. The structural system shown in Fig. 8 is analysed. It consists of a single span of deck concrete slab (up to span longitudinal symmetry axis) and adjacent truss girder member, both of the length *r* (cross-beam spacing). The composite deck is connected to the girder with a "connecting member" of length *d*. The member is assumed to have cross-sectional properties just like steel cross-beam. The length *d* equals the distance between the outermost shear connector of cross-beam and the longitudinal centre plane of a truss girder.

In a real structure the "connecting member" consists of steel cross-beam and stiffener of the truss flange adjacent to the deck (Fig. 5). Its moment of inertia in horizontal plane is smaller than

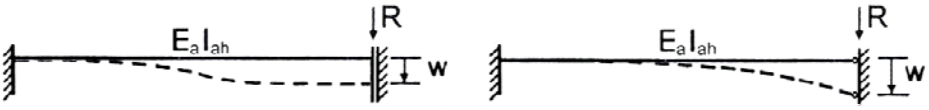

Fig. 9 Fixed-fixed (left) and fixed-hinged (right) boundary conditions for the "connecting member"

I_{ah}. To take it into account an additional flexibility is introduced. Namely it is assumed that the response of the "connecting member" to the force N is an average of the two cases of boundary conditions: fixed-fixed and fixed-hinged. The conditions are shown in Fig. 9, left and right, respectively.

In the system shown in Fig. 8 the force N is carried to support by truss girder member and concrete slab. The extent of joint action of the two members is governed by flexural stiffness in horizontal plane of the "connecting member" of length d.

For the system shown in Fig. 8 the difference of forces N and P_a is expressed as a function of the difference on elongations of the flange member adjacent to the deck (Δl_a) and the concrete slab (Δl_c)

$$\mathrm{N} - \mathrm{P_a} = \frac{\kappa \cdot \mathrm{E_a} \cdot \mathrm{I_{ah}}}{\mathrm{d}^3} \cdot \left(\Delta \mathrm{l_a} - \Delta \mathrm{l_c}\right). \tag{8}$$

where κ is 12 for the fixed-fixed boundary conditions (Fig. 9, left) and 3 for the and fixed-hinged boundary conditions (Fig. 9, right).

The equilibrium of forces (N, P_a, P_c) must occur in the same time and both elongations (Δl_a, Δl_c) are described by Hooke's law.

Equivalent cross-sectional area of truss flange must provide equality of its elongation and the elongation of the truss flange as part of the system shown in Fig. 8. It means that

$$\frac{\mathrm{N} \cdot \mathrm{r}}{\mathrm{E_a} \cdot \mathrm{A_{a\,equ}}} = \frac{\mathrm{P_a} \cdot \mathrm{r}}{\mathrm{E_a} \cdot \mathrm{A_a}} \tag{9}$$

Thus the equivalent cross-sectional area ($A_{a\,equ}$) of the flange member adjacent to the deck is:

– in the case of fixed-fixed boundary conditions (κ=12)

$$\mathrm{A_{a,ff}} = \frac{\mathrm{d}^3 \cdot \mathrm{A_a} \cdot \beta \cdot \mathrm{A_c} + 12 \cdot \mathrm{I_{ah}} \cdot \mathrm{r} \cdot \left(\beta \cdot \mathrm{A_c} + \mathrm{A_a}\right)}{\mathrm{d}^3 \cdot \beta \cdot \mathrm{A_c} + 12 \cdot \mathrm{I_{ah}} \cdot \mathrm{r}} \tag{10}$$

– in the case of fixed-hinged boundary conditions (κ=3)

$$\mathrm{A_{a,fh}} = \frac{\mathrm{d}^3 \cdot \mathrm{A_a} \cdot \beta \cdot \mathrm{A_c} + 3 \cdot \mathrm{I_{ah}} \cdot \mathrm{r} \cdot \left(\beta \cdot \mathrm{A_c} + \mathrm{A_a}\right)}{\mathrm{d}^3 \cdot \beta \cdot \mathrm{A_c} + 3 \cdot \mathrm{I_{ah}} \cdot \mathrm{r}} \tag{11}$$

where: $A_{a,ff}$, $A_{a,fh}$-equivalent cross-sectional area (m^2) of flange member adjacent to the deck obtained for the fixed-fixed and fixed-hinged boundary conditions, respectively, A_c-half of cross-sectional area of the concrete slab (m^2), E_c-elastic modulus of concrete (kPa), E_a-elastic modulus of steel (kPa), $\beta = \frac{\mathrm{E_c}}{\mathrm{E_a}}$, I_{ah}-moment of inertia of steel cross-beam in horizontal plane (m^4).

The mean value of the equivalent cross-sectional area $A_{a,m}$ is

$$A_{a,m} = \frac{A_{a,ff} + A_{a,fh}}{2} \tag{12}$$

In this way the $A_{b,m}$ of the bottom flange of the truss girder shown in Fig. 5 is computed.

Thus the modified moment of inertia of a truss bridge span is

$$I_{a.m} = 2 \cdot \left(I_t + A_t \cdot z_{t,m}{}^2 + I_b + A_{b,m} \cdot z_{b,m}{}^2 \right) \tag{13}$$

where: $A_{b,m}$-average cross-sectional area of bottom flange (m^2) accounting for joint action of truss girders and steel-concrete composite deck, computed according to Eq. (12), $z_{t,m}$, $z_{b,m}$-distance from the truss centre of gravity to the centre of gravity of top and bottom flange, respectively (m), computed for the bottom flange area equal to $A_{b,m}$.

Bracing members of trusses provide smaller shear stiffness in comparison to webs of plate girders. Hence, effective moment of inertia of truss girder is smaller than given in Eq. (13). The difference depends on truss static scheme-type of supports and loading. In the case of bridge truss girders, a simply supported and uniformly loaded beam is a representative scheme. So the moment of inertia of a truss bridge span accounting for the actual shear stiffness of truss girders is (Pałkowski 2001)

$$I_{a.r} = \frac{I_{a.m}}{1 + \frac{48}{5} \cdot \frac{E_a \cdot I_{a.m}}{(2 \cdot S_v) \cdot L_t{}^2}} \tag{14}$$

where: $I_{a.r}$-moment of inertia of truss bridge span accounting for joint action of the bridge deck and girders as well as actual shear stiffness of the truss girders provided by diagonal bracing (m^4), L_t-truss girder theoretical length (m), S_v-shear stiffness for a single truss girder, $2 \cdot S_v$-shear stiffness for a truss bridge span made of two girders.

In the case of a truss girder with parallel flanges and "*W*" bracing, its shear stiffness equals (Pałkowski 2001)

$$S_v = E_a \cdot A_d \cdot \sin^2(\alpha) \cdot \cos(\alpha) \tag{15}$$

where: α is an inclination angle of diagonal bracing (measured with respect to horizontal plane), A_d-cross-sectional area of bracing diagonal of a truss girder (m^2), if the area of bracing diagonals vary the average is assumed.

The computation results of the refined analytical method are put together in Table 6.

Table 6 The computation results of the advanced analytical method

Parameter	Units	Value
$I_{a.s}$	m^4	3.007
$A_{b,m}$	m^2	0.0510
$z_{b,m}$	m	3.55
$z_{t,m}$	m	5.30
$I_{a.m}$	m^4	1.625
A_d	m^2	0.0165
S_v	kN	$1.29 \cdot 10^6$
$I_{a.r}$	m^4	1.664

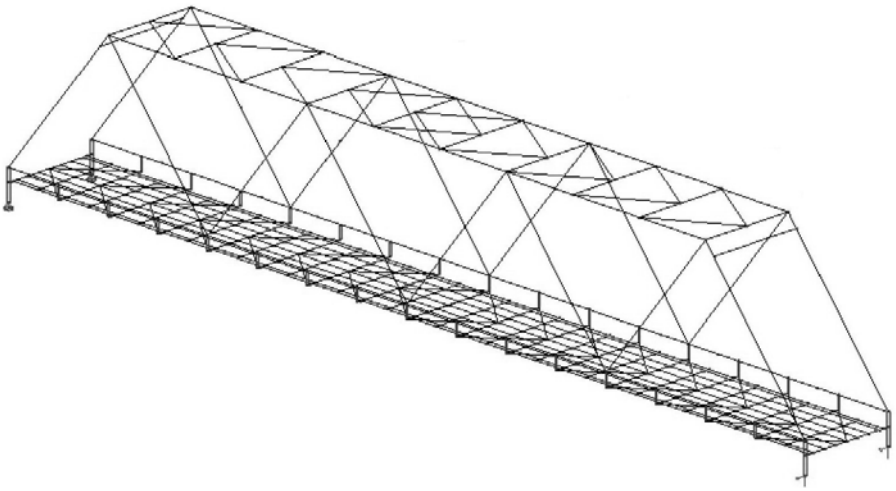

Fig. 10 Computational model of finite element method

Table 7 Computed displacements of bottom flange nodes

Node number	Displacement $u_{i\,FEM}$ [mm]
1	9.43
2	13.35
3	9.29

6. FEM assessment of span moment of inertia

Finite element method, implemented in the Autodesk Robot package (Autodesk Robot 2013), was used to create numerical model of the bridge span presented in the Chapter 3. The model is shown in Fig. 10. Structure dimensions were assumed as in the design documentation and cross-sectional data-as in Table 1.

The computational model consists of beam elements, that model truss girders, transverse beams, wind bracings, and shell elements modelling RC slab. The shell elements are placed at the level of RC slab mid-plane. Kinematic constraints are applied to appropriate pairs of nodes of cross-beams and truss bottom flanges to ensure compatibility of displacements. They are shown in Fig. 10 as short vertical elements connecting girders and deck.

The FEM model respects eccentricity of bottom flange and different levels of neutral axes of steel cross-beams, composite cross-beams, and slab mid-plane.

Based on the models the displacements of truss bottom flange nodes under test loading (Fig. 6) were computed. They are put in Table 7.

The equivalent moment of inertia I_{FEM} for the numerical results ($u_{i\,FEM}$) was computed with an aid of a result search analysis available in a spreadsheet. The following condition was applied

$$\sum_{i=1}^{3}\left(u_{i\,FEM}-u_{i\,est}\right)^2=\min \tag{16}$$

where: $u_{i\,FEM}$-computed displacement of nodes of truss bottom flange based on the numerical analysis, $u_{i\,est}$-displacement of the respective three points located on a simply supported beam of

Table 8 Computed displacements for the equivalent moment of inertia I_{FEM}

Nodal forces P_j (kN)	Displacements $u_{ij\,est}$ (mm) at the respective points on the equivalent beam		
	1 ($¼ \cdot L_t$)	2 ($½ \cdot L_t$)	3 ($¾ \cdot L_t$)
P_0=305.4	0.00	0.00	0.00
P_1=742.8	2.99	3.65	2.32
P_2=839.6	4.13	6.00	4.13
P_3=736.4	2.30	3.62	2.96
P_4=315.8	0.00	0.00	0.00
Total ($u_{i\,est}$)	9.42	13.27	9.41

Table 9 Equivalent moments of inertia resulted from application of different methods

Result source	Symbol	I (m^4)	$\frac{I}{I_{\exp}}$
Experiment	I_{exp}	2.154	1.00
Simplified analytical method	$I_{a.s}$	3.007	1.40
Refined analytical method	$I_{a.r}$	1.664	0.77
Finite element method	I_{FEM}	1.886	0.88

the bridge span length (described according to Eq. (4)).

The obtained equivalent moment of inertia equals I_{FEM}=1.886 m^4. The computed displacements of the respective points (1, 2, 3) of an equivalent simply supported beam are put together in Table 8.

7. Comparison of computation results

An equivalent moment of inertia of a through truss bridge span was estimated with an aid of four different methods: experimental, simplified analytical, refined analytical and numerical. The computation results are put together in Table 9.

It can be seen from Table 9 that refined analytical method and the finite element method give similar results-the span equivalent moment of inertia is underestimated by 12÷23%. The simplified analytical method provides a 40% overestimation of the moment of inertia.

8. Conclusions

The equivalent moment of inertia of a truss bridge span was estimated on the basis of test loading results. A simply supported beam of constant flexural stiffness was used as a model and the least squares method was applied to find the moment of inertia that provides the best agreement with recorded displacements of the truss bridge span.

The moment of inertia was estimated using simplified and refined analytical methods. The simplified method assumes that the moment of inertia of a bridge span depends only on truss girders which are treated as web-less plate girders. The refined method takes into account joint

action of a bridge deck and girders as well as actual shear stiffness provided by diagonal bracing.

Finite element model was created to estimate the bridge span moment of inertia. It consists of beam elements modelling truss members, steel cross-beams and bracing members as well as shell elements modelling deck concrete slab.

The simplified analytical method should not be applied to assess the equivalent moment of inertia of a truss bridge span. However the refined analytical method provides the accuracy of estimation similar to the finite element method. The discrepancies of results provided by the two methods can be reduced by further refining of the analytical method i.e. accounting for dimensions of truss joints and rigidity of wind bracing.

The refined analytical method and the finite element method underestimate the moment of inertia of the tested truss bridge span. It complies with the fact that actual flexural stiffness of bridge spans is usually underestimated by computational models.

The refined analytical method is applicable to preliminary design of trussed structures and rapid assessment of flexural stiffness of existing truss bridge spans.

Acknowledgements

The support of the 503213/01/12/DS-PB/0409/14 grant of the Ministry of Science and Higher Education of Republic of Poland is kindly acknowledged.

References

Autodesk Robot (2013) <http://usa.autodesk.com/adsk/servlet/index?siteID=123112&id= 13093279>

Chen, W.F. and Duan, L. (2013), *Handbook of International Bridge Engineering*, CRC Press.

Gao, Z. (2012), "Zhengzhou Yellow River Road-Cum-Railway Bridge, China", *Stahlbau*, **81**, 151-155.

Hu, N., Dai, G.L., Yan, B.and Liu, K. (2014), "Recent development of design and construction of medium and long span high-speed railway bridges in China", *Eng. Struct.*, **74**, 233-241.

Li, Z.X., Zhou, T.Q., Chan, T.H.T. and Yu, Y. (2007), "Multi-scale numerical analysis on dynamic response and local damage in long-span bridges", *Eng. Struct.*, **29**, 1507-1524.

Pałkowski, S. (2001), *Konstrukcje Stalowe. Wybrane Zagadnienia Obliczania i Projektowania* (Steel Structures. Some Aspects of Computation and Design), PWN, Warsaw, Poland.

Reintjes, K.H. (2009), "Das Zügelgurt-Fachwerk über die Mulde in Wurzen-eine Revision nach Entwurf und Ausführung (The Bridle-Chord Truss Bridge Across the River Mulde near Wurzen, Germany-a Review after Design and Construction)", *Stahlbau*, **78**, 188-196.

Siekierski, W. (2014), "Composite deck in 2D modelling of railway truss bridge", *Baltic J. Road Bridge Eng.*, **9**(2), 115-122.

Unsworth, J.F. (2010), *Design of Modern Steel Railway Bridges*, CRC Press.

Xia, C. and Zhong, T. (2011), "Numerical analysis of the Nanjing Dashengguan Yangtze River Bridge subjected to non-uniform seismic excitations", *J. Mech. Sci. Tech.*, **25**(5), 1297-1306.

Zhang, Y.Z. and Zhang, M. (2011), "Structure and behavior of floor system of two super high-speed railway Changjiang Composite Bridges", *J. Cent. South Univ. Technol.*, **18**, 542-549.

Zheng, P. and Dai, G. (2013), "A comparative study on static properties of a three-main-truss and three-cable-plane cable-stayed bridge", *J. Eng. Des. Tech.*, **11**(2), 207-220.

CC